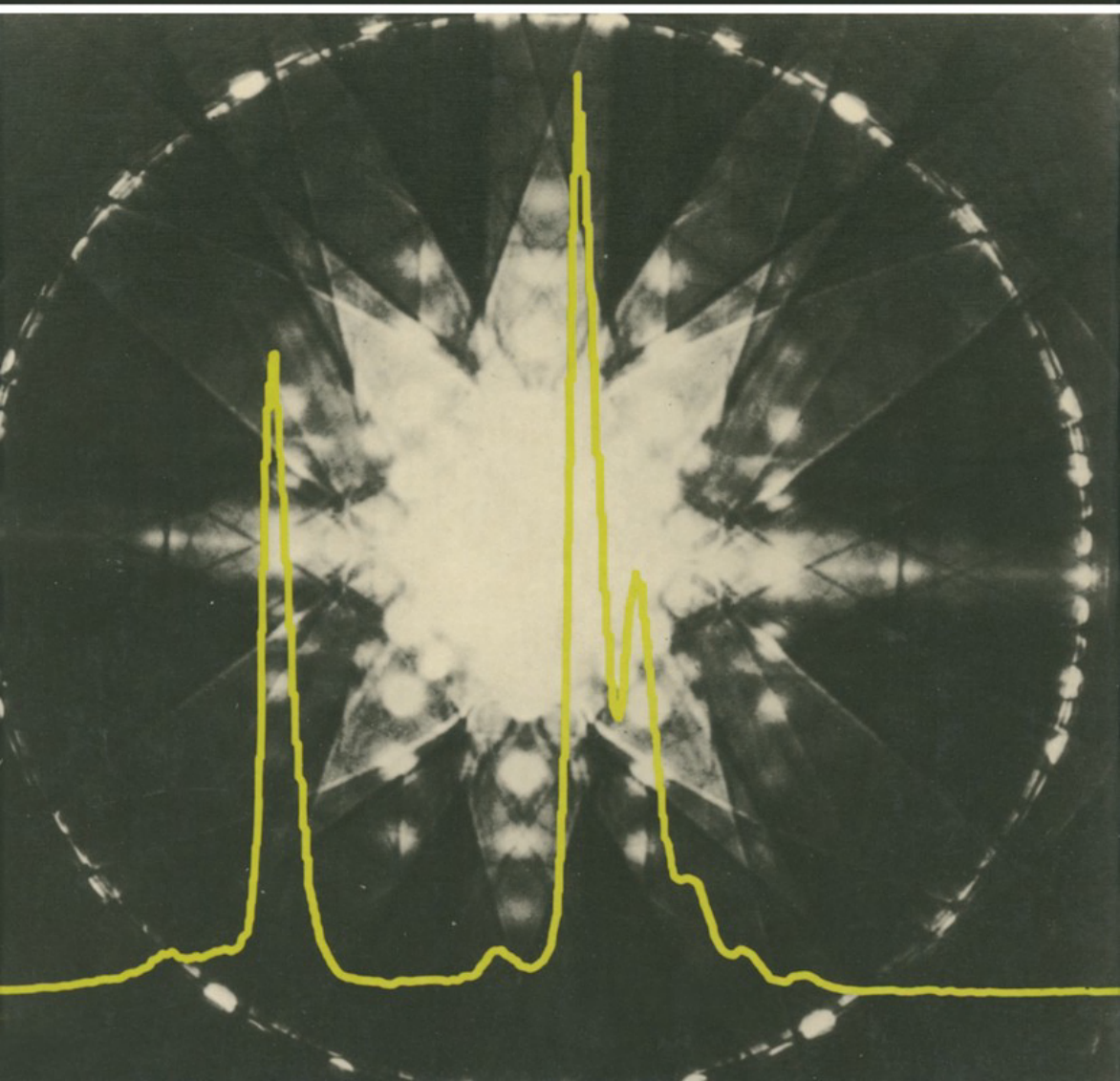


ELECTRON BEAM ANALYSIS OF MATERIALS

M.H. LORETTO



**ELECTRON BEAM
ANALYSIS OF
MATERIALS**

**ELECTRON BEAM
ANALYSIS OF
MATERIALS**

M. H. Loretto

*Professor of Materials Science
University of Birmingham*

LONDON
NEW YORK
**Chapman
and Hall**

*First published 1984 by
Chapman and Hall Ltd
11 New Fetter Lane, London EC4P 4EE
Published in the USA by
Chapman and Hall
733 Third Avenue, New York NY 10017*

© 1984 M.H. Loretto

Softcover reprint of the hardcover 1st edition 1984

Printed in Great Britain at the University Press, Cambridge

ISBN-13: 978-94-010-8944-9

This title is available in both hardbound and paperback editions. The paperback edition is sold subject to the condition that it shall not, by way of trade or otherwise, be lent, re-sold, hired out, or otherwise circulated without the publisher's prior consent in any form of binding or cover other than that in which it is published and without a similar condition including this condition being imposed on the subsequent purchaser.

All rights reserved. No part of this book may be reprinted, or reproduced or utilized in any form or by any electronic, mechanical or other means, now known or hereafter invented, including photocopying and recording, or in any information storage and retrieval system, without permission in writing from the Publisher.

British Library Cataloguing in Publication Data

Loretto, M.H.

Electron beam analysis of materials.

1. Materials – Testing 2. Electron beams
– Industrial applications

I. Title

620.1'12 TA410

ISBN-13: 978-94-010-8944-9

Library of Congress Cataloging in Publication Data

Loretto, M.H.

Electron beam analysis of materials.

Bibliography: p.

Includes index.

1. Materials – Analysis. 2. Electron beams –
Industrial applications. 3. Electron microscopy.

I. Title.

TA417.23.L67 1984 620.1'127 84–11351

ISBN-13: 978-94-010-8944-9 e-ISBN-13: 978-94-009-5540-0

DOI: 10.1007/978-94-009-5540-0

CONTENTS

<i>Preface</i>	vii
<i>Acknowledgements</i>	viii
1 Introduction to electron beam instruments	1
1.1 Introduction	1
1.2 Basic properties of electron emitters	1
1.3 Electron optics, electron lenses and deflection systems	7
References	18
2 Electron–specimen interactions	19
2.1 Introduction	19
2.2 Elastically scattered electrons	19
2.3 Inelastically scattered electrons	24
2.4 Generation of X-rays	26
2.5 Generation of Auger electrons	35
2.6 Generation of electron beam induced current and cathodoluminescence signals	37
References	38
3 Layout and operational modes of electron beam instruments	39
3.1 Transmission electron microscopy	39
3.2 Scanning electron microscopy	44
3.3 Scanning transmission electron microscopy	50
3.4 Auger electron spectroscopy	53
3.5 Electron microprobe analysis	56
3.6 X-ray spectrometers	57
3.7 Electron spectrometers	61
References	64
4 Interpretation of diffraction information	65
4.1 Introduction	65
4.2 Analysis of electron diffraction patterns	65

4.3 Interpretation of diffraction maxima associated with phase transformations and magnetic samples	101
4.4 Interpretation of diffraction patterns from twinned crystals	108
4.5 Interpretation of channelling patterns and backscattered electron patterns in scanning electron microscopy	109
References	112
5 Analysis of micrographs in TEM, STEM, HREM and SEM	113
5.1 Introduction	113
5.2 Theories of diffraction contrast in transmission electron microscopy	114
5.3 Analysis of images in transmission electron microscopy	119
5.4 Influence of electron optical conditions on images in TEM and STEM	143
5.5 Interpretation of high resolution electron microscopy images	144
5.6 Interpretation of scanning electron microscopy images	147
References	151
6 Interpretation of analytical data	153
6.1 Interpretation of X-ray data	153
6.2 Interpretation of data from thin samples	153
6.3 Interpretation of X-ray data from bulk samples	162
6.4 Interpretation of electron energy loss spectra	163
6.5 Interpretation of Auger spectra	169
6.6 Spatial resolution of analysis	175
References	177
Appendix A The reciprocal lattice	179
Appendix B Interplanar distances and angles in crystals. Cell volumes. Diffraction group symmetries	184
Appendix C Kikuchi maps, standard diffraction patterns and extinction distances	189
Appendix D Stereomicroscopy and trace analysis	198
Appendix E Tables of X-ray and EELS energies	200
<i>Index</i>	209

PREFACE

The examination of materials using electron beam techniques has developed continuously for over twenty years and there are now many different methods of extracting detailed structural and chemical information using electron beams. These techniques which include electron probe microanalysis, transmission electron microscopy, Auger spectroscopy and scanning electron microscopy have, until recently, developed more or less independently of each other. Thus dedicated instruments designed to optimize the performance for a specific application have been available and correspondingly most of the available textbooks tend to have covered the theory and practice of an individual technique. There appears to be no doubt that dedicated instruments taken together with the specialized textbooks will continue to be the appropriate approach for some problems. Nevertheless the underlying electron-specimen interactions are common to many techniques and in view of the fact that a range of hybrid instruments is now available it seems appropriate to provide a broad-based text for users of these electron beam facilities. The aim of the present book is therefore to provide, in a reasonably concise form, the material which will allow the practitioner of one or more of the individual techniques to appreciate and to make use of the type of information which can be obtained using other electron beam techniques.

The techniques which are covered in this book are electron diffraction, including convergent beam diffraction, conventional and high resolution transmission electron microscopy, scanning and scanning transmission electron microscopy, electron energy loss spectroscopy, Auger spectroscopy and X-ray microanalysis. In order to provide the necessary background information, the first chapter deals with electron optics at a very elementary level, the second chapter covers the factors which are important in influencing electron-specimen interactions and thus in generating the various signals which are detected. The third chapter covers the layout and mode of operation of the various instruments.

The theory has been kept to a minimum and references are given where appropriate to more detailed treatments. The book is aimed primarily at research scientists but it is written at a level appropriate to research students and final year undergraduates.

ACKNOWLEDGEMENTS

Many research students and colleagues have commented critically on earlier drafts of the book and I would like to take this opportunity of thanking them for their interest and help. I would also like to thank Miss Tina Salliss for her patience and skill in turning my difficult-to-read script into a typescript and Mrs E. Fellows for producing line diagrams and micrographs from originals of somewhat dubious quality. Finally, I would like to acknowledge the various authors and journals for allowing me to reproduce various figures in this book. These are acknowledged individually in the appropriate figure legends.

1

INTRODUCTION TO ELECTRON BEAM INSTRUMENTS

1.1 INTRODUCTION

Many electron beam instruments, which have been developed more or less independently of each other, are now being used either as individual or as hybrid instruments. Partly because the individual instruments have been developed separately, and partly because some instruments generate data which are more immediately interpretable, the fundamental relationships between the techniques and instruments tend to be obscured. The aims of this book are firstly to describe and discuss many of the modern instruments in a way which makes manifest the common ground between them and which highlights the advantages, disadvantages and fields of application of each instrument, so that their roles in materials science are clearly defined. Secondly, the book aims to provide the basic interpretation of the information which is available from each instrument, without attempting to present a detailed discussion of the underlying theory.

All of these instruments which are used to characterize materials have some similar basic requirements: an operating vacuum, although this varies between 10^{-3} and 10^{-10} Torr; an electron source; electron lenses for forming an electron probe; deflection systems for defining the probe position, and if necessary for rastering the probe; detectors to detect the signals, and an image-forming system. A discussion of vacuum systems is outside the scope of this book and in the introductory chapter, electron sources, electron lenses and deflection systems will be discussed; Chapter 2 deals with the basic science of electron-specimen interactions, the various instruments covered in the book are described in Chapter 3 together with the detection and processing of the many signals generated by electron-specimen interactions. The interpretation of signals is discussed in some detail in Chapters 4, 5 and 6. The appendices contain some essential data which are frequently required in interpreting the signals.

1.2 BASIC PROPERTIES OF ELECTRON EMITTERS

Electron sources in electron beam instruments are required to provide either a large total current in a beam of about $50\ \mu\text{m}$ diameter, as in the

case of low magnification transmission electron microscopy, or a high intensity probe of electrons as small as 0.5 nm in diameter, as in several scanning instruments. These requirements are not easily met by one type of electron source and sources have been developed which are more suitable for one type of application than for another. There are three basically different types of electron source available: the conventional tungsten hairpin filament (which can be modified to be a pointed tungsten filament), a lanthanum hexaboride crystal (LaB_6) and a field emission source.

In the presence of a suitable potential, electrons can be extracted from a source either by thermionic emission, in which the thermal energy of the electrons is sufficient for them to overcome the potential energy barrier (the work function) so that they can escape from the source, or by field emission which involves electron tunnelling so that the width of the potential barrier allows the quantum tunnelling of electrons so enabling them to escape from the source. Electron tunnelling requires very high field strengths and it is possible to operate sources in a hybrid manner so that the electron emission occurs at a lower field strength than is necessary for cold field emission and at a lower temperature than is necessary for thermionic emission, so that thermal field emission takes place. Before looking at the details of the different types of source it is useful to look at the characteristics of sources since it is these characteristics, the brightness, the stability, the size, the energy spread and the coherence, which define the performance of the various sources.

(a) Source brightness

The source brightness, β_s , is defined as the current density per unit solid angle and is measured in $\text{A cm}^{-2} \text{sr}^{-1}$. The brightness, which increases linearly with increase in accelerating voltage, determines the total current which can be focussed onto the specimen and thus determines the current in the small probes necessary in scanning instruments. Thus the maximum (theoretical) current, I_{th} , in a probe diameter d formed from a source of brightness β_s is given by [1]

$$I_{\text{th}} = \beta_s (\pi^2 \alpha^2 d^2) / 4 \quad (1.1)$$

where α is the semiangle of the probe-forming lens. Both the spherical aberration, caused by the probe-forming lens, and diffraction by the final aperture give rise to discs of confusion so limiting the current in a probe (see Section 1.3). The maximum current in a probe, subject to these two additional factors, is then given by

$$I_{\text{max}} = \frac{3\pi^2 \beta_s}{16} \left(\frac{d^{8/3}}{C_s^{2/3}} - \frac{4}{3} (1.22\lambda)^2 \right) \quad (1.2)$$

where C_s is the spherical aberration coefficient of the lens, λ the electron wavelength and d the probe diameter. For a fixed electron optical system

β_s is the only variable parameter and for the three types of electron sources, the conventional tungsten hairpin filament, the LaB_6 filament and the single crystal tungsten field emitter, the brightness varies roughly in the ratios 1, 10 to about 10^4 .

(b) Source stability

Any variation of emission current with time is undesirable, but all electron sources suffer from short or long term instabilities to varying extents. Short term stability is important in scanned images, in order to avoid image flicker, and in scanned X-ray, Auger or other analytical applications where the level of the signal is significant. The tungsten hairpin filament is generally remarkably stable, with emission varying by less than $\pm 1\%$ over many hours, once any initial instabilities disappear. Typically these instabilities last for only a few minutes with a new filament and for an even shorter time when an old filament is switched on. It should be noted, however, that the steady emission current may change to a different steady current if the filament is switched off and on, and if a constant current is required over many hours, the filament should be left on even when specimens or film is changed. This requirement necessitates pre-pumped airlocks which are common in modern electron beam equipment. LaB_6 filaments are not quite as stable as the tungsten hairpin filaments but again, after the initial instabilities, the emission current is constant over tens of hours within $\pm 2\%$, unless the filament is overheated. Field emission sources are relatively unstable both over short time intervals – i.e. fractions of seconds – and over longer times, of the order of half an hour, and special operational modes are being increasingly introduced in order to compensate for these instabilities. These techniques are discussed in Section 1.2.1 where the layout of field emission sources is described.

The instability in the sources can be due to many causes: mechanical drift, ion bombardment of the filament by gas ions, adsorption of residual gases present in the microscope column, and whisker formation on the filament. The tungsten hairpin filament is not as sensitive to the vacuum level as are the LaB_6 and field emission sources; the hairpin filament requires a vacuum of better than about 10^{-3} Torr and it is nearly as stable at such a poor vacuum level as at a level of around 10^{-6} Torr which is required for a LaB_6 filament. The emission from a thermal field emission source requires a vacuum of the order of 10^{-7} Torr and a cold field emission source of about 10^{-10} Torr for stable operation, and in both cases the stability is better the better the vacuum.

(c) The source size

As discussed in Section 1.3 it is common practice to demagnify the electron source in order to reduce the significance both of lens aberrations and of non-homogeneous electron emission over the emitting area of the source.

In general it is accepted that a source should be used whose emitting area is greater than the largest area to be illuminated at any one time. Typical source sizes are roughly $50\ \mu\text{m}$ for a conventional tungsten hairpin filament, $1\ \mu\text{m}$ for a LaB_6 filament and about $5\ \text{nm}$ for a field emission tip.

(d) Energy spread of sources

If there is a significant energy spread in the electron beam then chromatic aberration (see Section 1.3) associated with the lenses will lead to image degradation in transmission electron microscopy (TEM) and to an increase in probe size in scanning instruments. The influence of an energy spread, ΔE , is proportional to $\Delta E/E_0$ where E_0 is the accelerating voltage. The energy spread is caused both by instabilities in the HT source and by the inherent spread in energies associated with thermionic and field emission. The HT stability at $100\ \text{kV}$ is typically 1 part in 10^6 leading to an energy spread of only $0.1\ \text{eV}$. On the other hand the energy spread associated with a thermionic source heated to about $2800\ \text{K}$ is around $3\ \text{eV}$, the energy spread for a LaB_6 filament is about $1\ \text{eV}$, for a cold field emission source it is around $0.5\ \text{eV}$ and for a thermal field emission source about $2\ \text{eV}$.

(e) Source coherence

The coherence of an electron source is a measure of the phase differences in the emitted beam and this controls the amount of interference which can take place between the direct and the various diffracted waves. For example the number of Fresnel fringes [3] formed in the image of a holey carbon film is very much higher for a microscope with a field emission filament than for a tungsten hairpin thermionic filament. This difference arises because the effective size of the source in a field emission tip is only about $5\ \text{nm}$ so that the emitted electrons are in phase, i.e. the source is coherent, whereas the source size is about $50\ \mu\text{m}$ for a tungsten hairpin filament.

The diameter of the specimen over which the illumination is coherent is given by λ/α where λ is the wavelength of the electrons and α is the semi-angle subtended at the specimen by the source. The coherence of a source is important for high resolution imaging (see Chapter 5) but is unimportant for all other applications discussed in the book.

1.2.1 Electron sources

(a) Conventional thermionic tungsten hairpin sources

A schematic diagram of a conventional tungsten hairpin source is shown in Fig. 1.1. The hairpin filament is heated to about $2800\ \text{K}$ by direct resistance heating and the surrounding grid, known as the Wehnelt cylinder, together

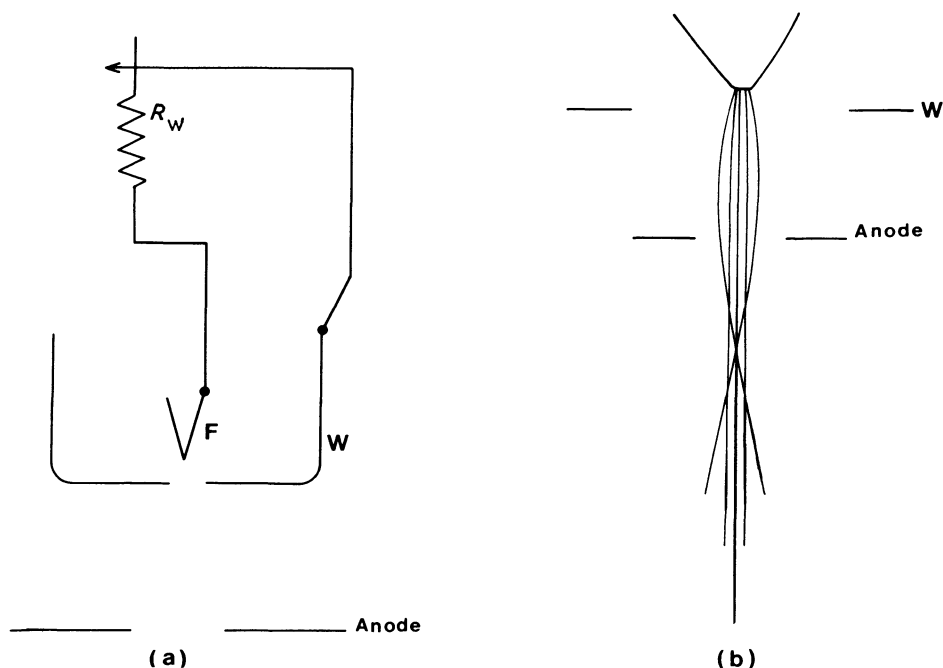


Fig. 1.1 Schematic diagram of a conventional tungsten thermionic source. (a) the filament F is at the accelerating potential of the instrument and is heated directly to about 2800 K. The Wehnelt cylinder W is biased by the potential drop across R_w (b) Schematic ray path showing focussing action.

with the anode, which is at earth potential, act as an electrostatic lens (see Section 1.3) forming an image of the region of the filament which is emitting electrons, just before or just beyond the anode aperture. This image of the filament is termed a crossover. The source size is about $50 \mu\text{m}$, and because of the self-biasing action of the gun (see Fig. 1.1) the stability is excellent.

Measurement and calculation show that for typical operating conditions at 100 kV the brightness of such a thermionic gun is about $3 \times 10^5 \text{ A cm}^{-2} \text{ sr}^{-1}$. This type of gun, when used in a modern transmission electron microscope, is capable of producing an electron probe in the transmission electron microscope (TEM) mode (see Section 1.3) with a diameter d of 40 nm with a current of about 1 nA and in the scanning transmission electron microscope (STEM) mode (see Section 1.3) with $d = 4 \text{ nm}$ and a current of about 0.05 nA. Thus, although the conventional tungsten filament is capable of providing the relatively large total current ($\approx 1 \mu\text{A}$) required for low magnification imaging in the TEM mode, it is not able to generate high intensity probes because of the inherent low brightness. Pointed single crystal thermionic tungsten filaments provide higher brightness sources than the hairpin filament but the recent

success of LaB_6 filaments, which offer a greater increase in brightness and longer life, suggests that these filaments are a more satisfactory compromise between the thermionic and the field emission sources.

(b) LaB_6 sources

Although the development of LaB_6 filaments has been slow they are now replacing the conventional filament in many electron beam instruments. This has become possible partly because the vacuum in microscopes has been improved (mainly to reduce electron-beam-induced contamination of specimens caused by the high residual hydrocarbon level in the specimen area) so that LaB_6 filaments can be operated successfully, and partly because of the simplified design of the modern LaB_6 filament assembly. Basically the only difference between the conventional assembly illustrated in Fig. 1.1 and a modern LaB_6 assembly is that extra pumping holes are present in the Wehnelt cap to ensure a better pumping speed near the LaB_6 tip. The brightness of a LaB_6 filament can be as high as $10^7 \text{ A cm}^{-2} \text{ sr}^{-1}$ at 100 kV which is an improvement of a factor of about thirty over the tungsten hairpin filament. If the LaB_6 filament is operated at a lower brightness, say a factor five to ten above that of a tungsten hairpin filament, the lifetime can be increased to about 1000 hours, i.e. about ten times that of the tungsten filament. The higher current obtainable in small probes and the comparable total current from LaB_6 and conventional tungsten filaments, for use in low magnification transmission electron microscopy, will lead to the gradual replacement of the conventional tungsten filament by LaB_6 .

(c) Field emission sources

A field emission source is usually a $\langle 111 \rangle$ orientation crystal of tungsten and the Wehnelt cylinder is raised to an extraction potential up to about 4 kV in order to cause emission from the tip of the crystal. The very high field around the tip focusses any gas ions present onto the tip and the consequent ion bombardment leads to short term instabilities in emission current. Thus the requirement for a high vacuum is clear but even at around 10^{-9} Torr the tip becomes contaminated so that the emission decreases and it is necessary to flash the tip periodically, i.e. to heat it up to drive off the adsorbed impurities.

In view of the short and long term instabilities in the emission, which influence any time-dependent signal, it is necessary to monitor the emission current (or a signal which is proportional to the emission) and compensate electronically for the fluctuations. This is usually done by using a signal derived from the (electrically isolated) aperture of the second condenser lens; for example the brightness of a scanning image can be scaled to compensate for changes in this current.

Table 1.1 Summary of the important properties of available electron sources.

Source	Brightness ($\text{A cm}^{-2} \text{sr}^{-1}$)	Stability(%)	Source size	Energy spread (eV)
Tungsten	3×10^5	~ 1	$50 \mu\text{m}$	3
LaB_6	3×10^6	~ 2	$1 \mu\text{m}$	1
Cold field emission	10^9	~ 5	5 nm	0.5
Thermal field emission	10^9	~ 5	5 nm	2

The brightness of a cold or thermal emission source can be about 10^4 times that of a conventional tungsten filament. Because of the high brightness of field emission sources they are preferred in scanning instruments which require electron probes of 0.5 nm diameter but the small source size and associated small total current means that these sources are not ideal for low magnification transmission electron microscopy.

The important characteristics of the various electron sources are summarized in Table 1.1.

1.3 ELECTRON OPTICS, ELECTRON LENSES AND DEFLECTION SYSTEMS

1.3.1 Introduction

In this section a brief account will be given of the principles which underlie the operation of lenses in electron beam instruments and some important equations will be quoted so that the operation and limitations of probe-forming lenses, image-forming lenses and lenses used to collect and separate electrons of different energies may be understood. It is necessary to have at least this background in order to appreciate the operation of the various instruments discussed in Chapter 3 but it is outside the scope of this book to deal with the relevant electromagnetic theory; references are given at the end of this chapter to books which deal with this basic theory.

Electron lenses in electron microscopes are generally electromagnetic but the biased electron gun and lenses used in Auger spectrometers, and in some electron spectrometers attached to electron microscopes, are electrostatic lenses. The action and properties of electron guns are discussed in Section 1.2 of this chapter and a brief account of electrostatic lenses is given in Section 1.3.3.

1.3.2 Electron optics

The action of a magnetic field on an electron is described by the well-known right hand rule where the thumb, first and second fingers are used to re-

present the terms in a vector cross-product. The force \mathbf{F} which an electron of charge $-e$ experiences when travelling with a velocity \mathbf{v} , due to a magnetic field \mathbf{B} , is given by

$$\mathbf{F} = -e(\mathbf{v} \wedge \mathbf{B}) \tag{1.3}$$

and the magnitude of the force is then given by

$$F = Bev \sin \theta \tag{1.4}$$

where θ is the angle between \mathbf{B} and \mathbf{v} . If the initial velocity of an electron is divided into two components, v_p parallel to \mathbf{B} and v_o orthogonal to \mathbf{B} , then the value of v_p will be unchanged by \mathbf{B} (since θ will be zero) and the force resulting from \mathbf{B} and v_o will result in circular motion of the electron about

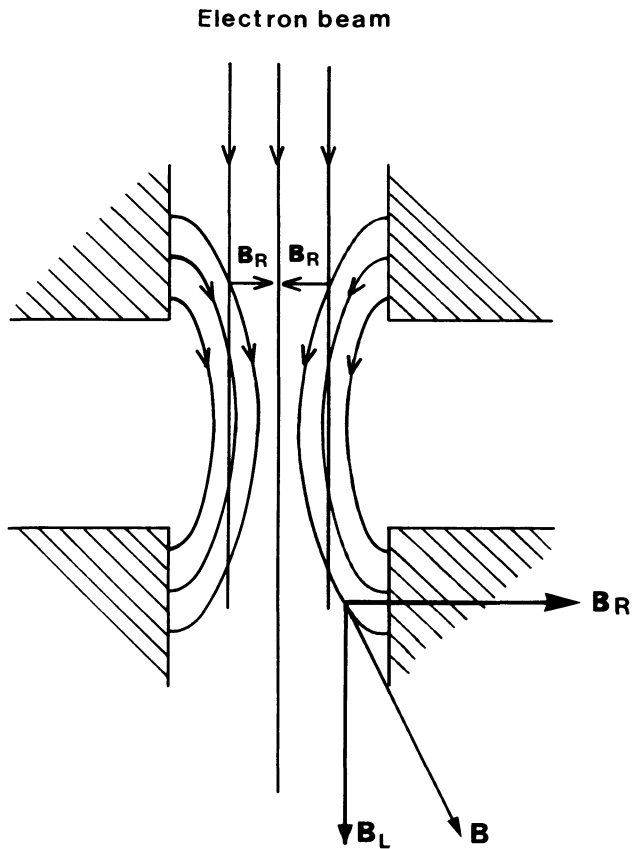


Fig. 1.2 Schematic diagram of the action of a cylindrical magnetic lens on the path of non-axial electrons. \mathbf{B}_R is the radial component and \mathbf{B}_L the longitudinal component of the field.

B. The radius of this motion is given by mv/eB and the resulting path of the electron will be a helix, the sum of the circular velocity and the unchanged longitudinal velocity, in the direction of the field.

If an inhomogeneous field is now considered we can see that it leads to a focussing action on electrons [2]. Thus, Fig. 1.2 shows, schematically, a cross section of a typical magnetic lens and the field produced by such a cylindrical lens is indicated in the figure. It can be considered to be made up of radial and longitudinal components, \mathbf{B}_R and \mathbf{B}_L respectively, which vary along the length of the lens, as shown schematically in Fig. 1.2. An electron entering the lens axially and precisely centrally will experience no force from the field in the lens, since the only component of the field in this part of the lens is \mathbf{B}_L which is parallel to \mathbf{v} . For an electron travelling along the axis of the lens, but not passing centrally through the lens, the situation is very different. Such electrons will interact with the radial component of the field \mathbf{B}_R , since \mathbf{B}_R is orthogonal to \mathbf{v} , and will experience a force of magnitude veB_R . This force causes the electron to change direction so that it now also experiences a force due to \mathbf{B}_L , the axial component of the field. The result of this is that the electron, which was initially travelling axially, spirals towards the centre of the lens, passes through the centre of the lens and then continues spiralling out from the centre before spiralling back. Such a trajectory is shown in Fig. 1.3.

It is easy to show [2] that the radial force on an electron is given by the expression

$$F = -\left(\frac{e^2}{4m}\right)B_L^2 r \quad (1.5)$$

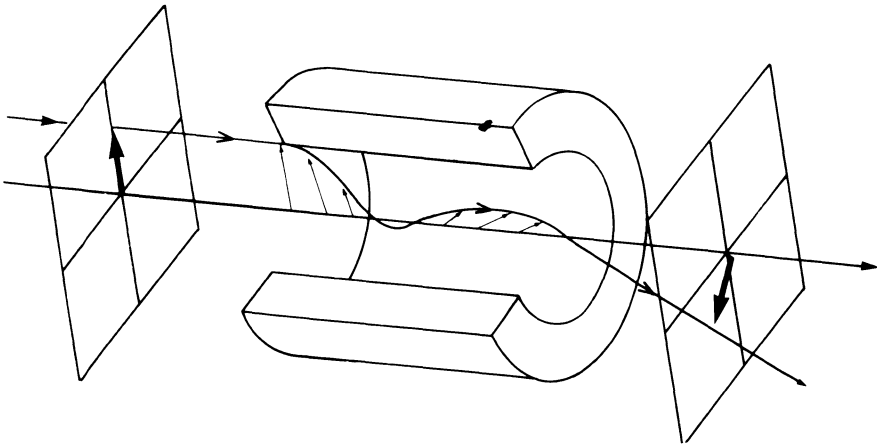


Fig. 1.3 Schematic diagram showing the trajectory of an electron through a magnetic lens.

where r is the radial distance of the axial electron from the centre of the lens. The force is proportional to r (hence the focussing action) and is directed towards the axis of the lens. Such lenses are always converging since F is independent of the sign of B_L .

The important parameters which describe electron trajectories within lenses, and which can be derived from the type of discussion presented above are: (1) the focal length of a lens and (2) the angular rotation of the image with respect to the object. If the axial extent of B_L is small, with respect to the focal length, then the (non-relativistic) thin lens formula for f , the focal length of the lens, can be shown [2] to be

$$\frac{1}{f} = \frac{300e}{8mc^2E} \int_{\text{gap}} B_L^2 dL \quad (1.6)$$

and the rotation of the image with respect to the object is given by

$$\theta = \left(\frac{300e}{8mc^2E} \right)^{1/2} \int_{\text{gap}} B_L dL \quad (1.7)$$

where E is the electron energy in electron volts, B_L is the longitudinal component of the field of the lens, m and e are the mass and charge (in esu) of the electron and c is the velocity of light. F is then given in centimetres and θ in radians. Since θ is controlled by B_L , successive lenses can be wound in opposite senses, such that θ_{total} is minimized or even reduced to zero.

The spherical aberration coefficient C_s of electromagnetic lenses is also calculable [2] and d_s , the diameter of the disc of confusion [3] referred to object space, is related to C_s by

$$d_s = 2C_s\alpha^3 \quad (1.8)$$

where α is the semiangle aperture of the lens. Similarly the chromatic aberration coefficient C_c is related to d_c , the radius of the disc in object space, by the relation

$$d_c = 2C_c\alpha \frac{\Delta E}{E_0} \quad (1.9)$$

where ΔE is the energy spread and E_0 is the accelerating voltage.

Typically C_s and C_c are of the same order as the focal length for a lens, and values for objective lenses in modern transmission electron microscopes are typically 1 to 2 mm and between 1 and 2 cm for scanning microscopes.

There is no convenient way with magnetic lenses to correct for spherical aberration and, unlike the case for optical microscopes, the only way to limit the influence of C_s on image quality and on probe diameter is to use an aperture to stop the lens down. Too small an aperture, however, degrades the information by diffraction from the aperture [3] and the diameter of

the diffraction disc d_d is given by

$$d_d = 1.22\lambda/\alpha \quad (1.10)$$

In probe-forming microscopes, where a suitable choice of the probe-forming aperture means that C_s is the limiting factor, it can be shown that there is an optimum aperture size for a probe of diameter d given by

$$\alpha_{\text{opt}} = \left(\frac{d}{C_s} \right)^{1/3} \quad (1.11)$$

Similarly, by combining equations (1.8) and (1.10) linearly, the resolution which is given by the diameter of the disc of confusion is given by

$$d_{\text{min}} = A\lambda^{3/4}C_s^{1/4} \quad (1.12)$$

The constant A is about unity. This equation can be used only as a rough guide for the resolution of an electron microscope since geometrical optics have been used. For $C_s = 2$ mm and 100 kV electrons this equation gives a resolution of about 3 Å.

1.3.3 Electron lenses

(a) Imaging and probe-forming lenses

The lenses in electron microscopes comprise a condenser system and an image-forming system and these lenses, together with the deflection coils (used for alignment and scanning) and apertures (which deliberately limit the collection or illumination angle) make up the electron optical systems which will be discussed here. Typical layouts of individual instruments are dealt with in Chapter 3.

The post-specimen lenses in TEM operate in a similar manner under all conditions of TEM because they are required to produce the total magnification simply by varying the power of one or more of the lenses. Of the imaging lenses it is the objective lens, which produces the first image of the object, which is required to be the most perfect lens. With modern 100 kV TEM/STEMs the values of C_s and C_c are typically about 2 mm, if 60° of specimen tilt is available, and 1.2 mm if only 15° is available. The value of C_s for high resolution electron microscopes (HREMs) operating at 600 kV–1 MV is about 2 mm even with 30° of tilt and because of the short wavelength the ultimate resolution is superior to that available in lower kV machines.

The condenser–objective lens systems in TEM/STEM instruments make most use of the flexibility of magnetic lenses, allowing a wide range of illuminating conditions to be used. The detailed modes of operation differ in different commercial instruments and the methods adopted in the Philips EM400T series will be used as a basis for the following description.

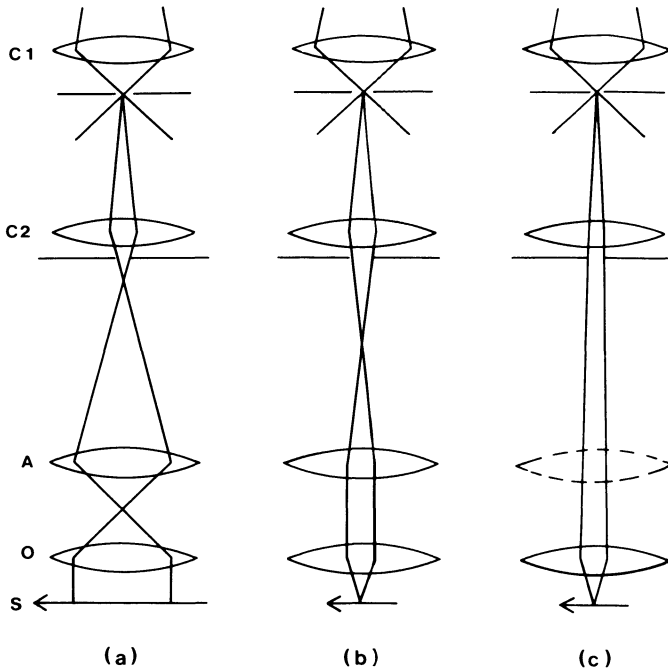


Fig. 1.4 Schematic ray diagrams in a transmission electron microscope. C1 and C2 are the first and second condenser lens, A is an auxiliary lens and O is the pre-field of the objective lens. S is the specimen. (a) illuminating system producing a near parallel beam at the specimen for TEM imaging; (b) production of convergent beam at specimen in TEM mode; (c) production of very small probe in TEM mode.

Fig. 1.4(a) shows schematically the illuminating system in a Philips EM400T operating in the TEM mode. In this mode the condenser-objective system provides a near-parallel beam at the specimen. This is achieved by operating the first condenser lens (C1) as a strong lens so that a demagnified image of the crossover from the electron gun is formed; the demagnification being of the order of a $100\times$ so that the $50\ \mu\text{m}$ crossover, typical of a tungsten hairpin filament gun is reduced to less than $1\ \mu\text{m}$ in diameter. The second condenser (C2), together with an additional auxiliary lens and the prefield of the objective lens, is used to project this image onto the specimen. In this type of microscope the specimen is immersed at the centre of the objective lens and the prefield plays an important part in the operation.

When C2 is overfocussed (Fig. 1.4(a)) a near-parallel beam illuminates a large area on the specimen. Typically the area can be as large as $25\ \mu\text{m}$ in diameter, for low magnification observations. This can be reduced to only about $40\ \text{nm}$ by suitably underfocussing C2, as shown in Fig. 1.4(b), where C2 and the auxiliary lens combine to produce a parallel beam, which is